

Visualization of Retroviral Replication in Living Cells Reveals Budding into Multivesicular Bodies

Nathan M. Sherer¹, Maik J. Lehmann¹, Luisa F. Jimenez-Soto¹, Alyssa Ingmundson¹, Stacy M. Horner¹, Gregor Cicchetti³, Philip G. Allen³, Marc Pypaert², James M. Cunningham⁴ and Walther Mothes^{1,*}

¹ Section of Microbial Pathogenesis and

² Department of Cell Biology, Yale University School of Medicine, 295 Congress Ave, New Haven, CT 06536, USA

³ Division of Hematology, Brigham and Women's Hospital, Boston, MA, 02115, USA

⁴ Howard Hughes Medical Institute and Division of Hematology, Brigham and Women's Hospital, Boston, MA, 02115, USA

* Corresponding author: Walther Mothes, waltherm. mothes@yale.edu

Retroviral assembly and budding is driven by the Gag polyprotein and requires the host-derived vacuolar protein sorting (vps) machinery. With the exception of human immunodeficiency virus (HIV)-infected macrophages, current models predict that the vps machinery is recruited by Gag to viral budding sites at the cell surface. However, here we demonstrate that HIV Gag and murine leukemia virus (MLV) Gag also drive assembly intracellularly in cell types including 293 and HeLa cells, previously believed to exclusively support budding from the plasma membrane. Using live confocal microscopy in conjunction with electron microscopy of cells generating fluorescently labeled virions or virus-like particles, we observed that these retroviruses utilize late endosomal membranes/multivesicular bodies as assembly sites, implying an endosome-based pathway for viral egress. These data suggest that retroviruses can interact with the vps sorting machinery in a more traditional sense, directly linked to the mechanism by which cellular proteins are sorted into multivesicular endosomes.

Key words: human immunodeficiency virus (HIV), imaging of viral replication, multivesicular body (MVB), murine leukemia virus (MLV), retroviral budding and assembly

Received 22 July 2003, revised and accepted for publication 26 August 2003

Retroviruses, such as the human immunodeficiency virus (HIV) and the murine leukemia virus (MLV), have until recently been thought to bud exclusively from the plasma membrane of infected cells (1–4). Budding is driven by the Gag polyprotein that alone is able to induce the formation and release of virus-like particles. Gag targets viral assem-

bly to cellular membranes, drives the formation of the immature capsid and induces budding away from the cytoplasm. Finally, in order to ultimately escape the cell, the viral Gag protein must recruit a variety of host cellular factors including members of the vacuolar protein sorting (vps) family [reviewed in (5–8)]. Failure to recruit these factors results in a 'late' phenotype in which particles are nearly assembled but remain tethered to the cell surface (9,10).

In yeast, class E vps proteins are required for the sorting of ubiquitinated cargo from the cell surface into the vacuole by driving the involution of endocytic membranes to bud small vesicles away from the cytoplasm into the degradative environment (11). The vps machinery is highly conserved throughout evolution and in mammalian cells contributes to the formation of a late endosomal compartment, the multivesicular body (MVB), characterized by its accumulation of intraluminal vesicles. A number of amino acid sequences within Gag as well as within the matrix proteins of a wide variety of enveloped viruses have been shown to interface with the vps and ubiquitination machineries. First, the P(T/S)AP motif, found in HIV and numerous enveloped viruses, interacts with TSG101/Vps23 (10). In yeast, cargo is ubiquitinated, recognized by Vps23 and sorted into the vacuole (12). Interestingly, Tsg101 binds to both ubiquitin and the PTAP motif of HIV Gag (10,13). Second, the PPXY motif, found within many enveloped viruses including MLV, is believed to interact with WW domains of the Nedd4 family of E3 ubiquitin ligases (14,15). Interactions with these proteins lead to the ubiquitination of Gag, a modification that is required for budding to occur (7,16,17). Although down-regulation of Tsg101 does not interfere with MLV budding, the release of both MLV and HIV can be blocked by over-expression of dominant negative mutants of Vps4 (10). Thus, the vps machinery contributes to the budding of these, if not all, enveloped viruses. Intriguingly, in the context of both MVB biogenesis and virus budding, the vps machinery exists as the only cellular machinery known to accomplish the sorting/budding of cellular-derived membranes away from the cytoplasm.

For most cell types, enveloped viruses are believed to bud from the surface of the cell and are predicted to recruit vps factors to the plasma membrane (8). Indeed, PTAP-dependent colocalization of the vps factor TSG101 to surface budding sites has been observed for the filovirus Ebola (18). However, surface budding cannot be the only mechanism of retroviral egress. HIV-infected

macrophages productively shed infectious virions into the supernatant despite the fact that these virions are not observed to bud from the cell surface (19). Instead, HIV has been shown to bud into MHC Class II compartments, modified MVBs capable of fusing with the plasma membrane to present antigen, simultaneously releasing any luminal contents including HIV virions and small vesicles termed exosomes (20–22). Currently, MVB-mediated viral egress is believed to be uniquely restricted to macrophages. Using a novel visual approach to monitor viral replication in living cells, we find that the ability of retroviruses to bud into MVBs can be observed in standard tissue culture cell lines previously believed to only support budding at the plasma membrane. Our data suggest that Gag targeting to late endosomal membranes may contribute to viral egress from these cells.

Results

A visual system to study retroviral replication in living cells

To monitor MLV replication in living cells, we have fused variants of the green fluorescent protein (green = GFP, cyan = CFP, yellow = YFP, red = RFP) to viral Gag to label the viral capsid. To label the viral envelope, we have inserted GFP variants into the extracellular domain of the Friend envelope protein (Env) (Figure 1A). The C-terminus of Gag allows for the attachment of proteins such as GFP (23,24). In fact, many virally acquired oncogenes are captured at the C-terminus of MLV Gag and are subsequently expressed as Gag-oncogene fusion proteins (25). Gag is normally expressed in the context of the Gag-Pol precursor protein. Because the attachment of GFP to Gag truncates Pol expression, the production of infectious GFP-labeled virions using Gag-GFP requires coexpression of wild-type Gag-Pol in order to package the viral enzymes encoded by the Pol region: reverse transcriptase (RT), integrase (IN) and protease (PR). When a plasmid encoding wild-type Gag-Pol was cotransfected with Gag-GFP at a ratio of 1 : 1 into 293 cells in the additional presence of plasmids encoding a viral RNA and Env, Gag-GFP was released into the supernatant as efficiently as wild-type Gag. Both proteins were identified by Western blotting in the fraction that sedimented through a 20% sucrose cushion (Figure 1B). Electron microscopy of 293 cells producing Gag and Env labeled virions revealed the incorporation of the GFP-fusion proteins into budding virions at expected positions either within the inner core of capsid or at the outer face of the viral envelope, respectively (Figure 1C). Most importantly, released viral particles retained high infectivity when Gag-GFP did not exceed 25% of all Gag molecules (Figure 1D). On average, that amounts to ~400 GFP-labeled molecules per particle and allows very bright labeling (Figure 1F). To further address the functionality of Gag-GFP, we asked if this protein could rescue MLV release when the late domain budding motif PPPY within

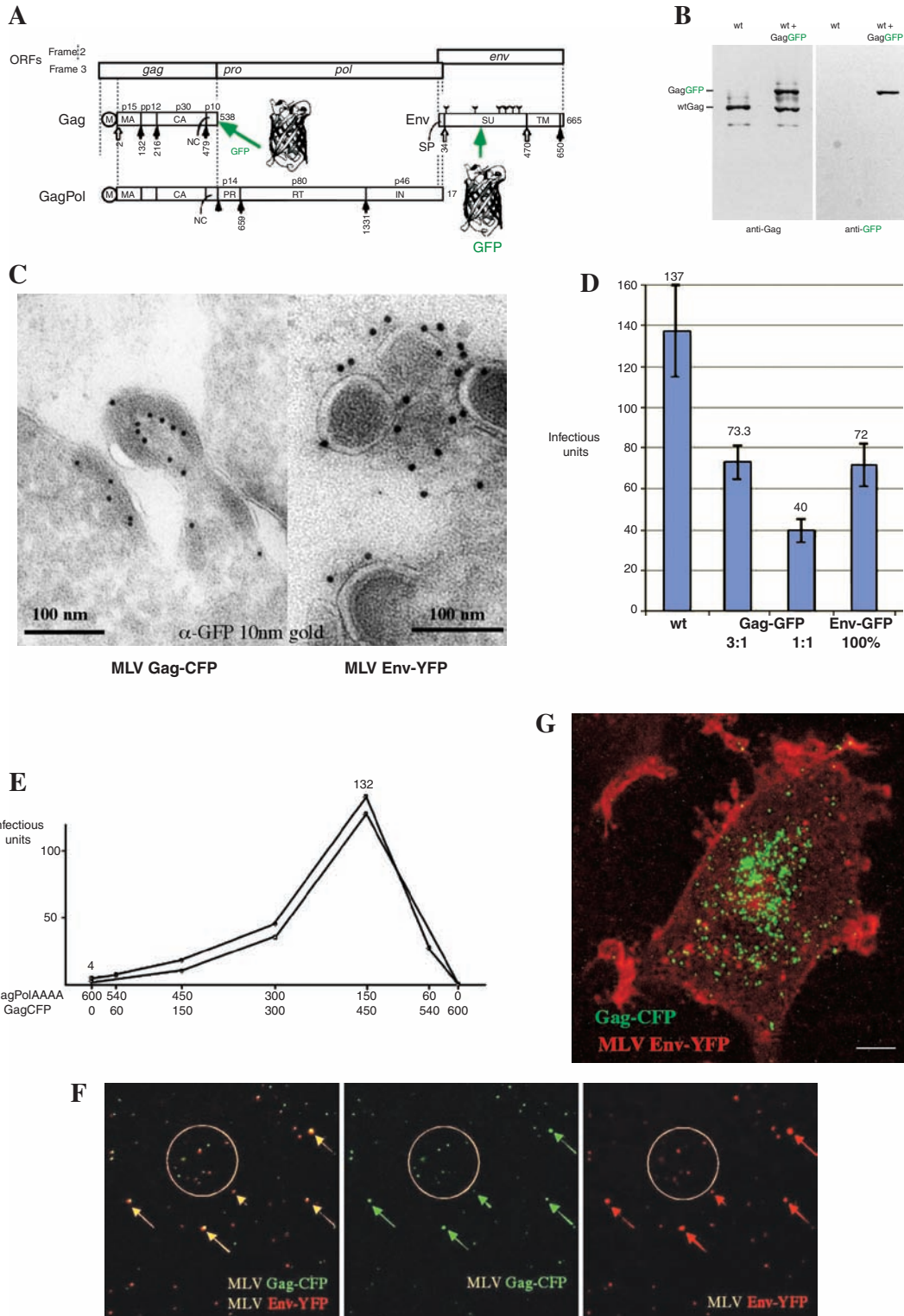
Figure 1: Generation of GFP-labeled infectious MLV virions.

(A) GFP variants were fused to the C-terminus of Gag to label capsid or inserted into the extracellular domain of Env to label the viral envelope. (B) Viruses were generated by transient transfection of plasmids encoding Gag-GFP and wild-type Gag-Pol (at a ratio of 1 : 1), as well as wild-type Env and an LTR containing LacZ as a reporter gene. The viral supernatant was centrifuged through a 20% sucrose cushion and blotted using antibodies against Gag (left panel) and GFP (right panel). (C) Electron micrographs of cryosections showing viruses budding from the surface of 293 cells. Infectious viral particles were labeled by cotransfection of either Gag-GFP (left panel) or Env-YFP (right panel). 10 nm immunogold labeling against GFP indicates the incorporation of the fusion proteins at expected sites within the virus. The size bar corresponds to 100 nm. (D) The infectivity of GFP-labeled virions was compared to that of wild-type MLV (lane 1) using LacZ staining. At a ratio of 1 : 3 Gag-GFP : Gag-Pol, the incorporation of Gag-GFP led only to a moderate drop in infectivity (lane 2). Expression of increasing amounts of Gag-GFP resulted in a further decrease in infectivity (lane 3). Therefore, typically, the ratio of Gag-GFP to Gag-Pol was kept at or below 1 : 3. 100% substitution of Env by Env-GFP led only to a moderate drop in infectivity in the pseudotyped virus when transferred into full-length virus [data not shown and (61)]. The number of LacZ⁺ cells as determined for wild-type MLV corresponds to a titer of 10⁶. (E) Gag-CFP rescues a budding deficient Gag-Pol containing virus. Pseudotyped virions produced in a 35-mm dish of 293 cells by transfection of 600 ng of each plasmid encoding wild-type Env, a LTR for LacZ and a budding impaired Gag-Pol in which the PPPY motif was mutated to AAAA (GagPolAAAA). Increasing the ratio of Gag-CFP to GagPolAAAA (while maintaining the sum of total Gag DNA at 600 ng) rescued the release of infectious particles as titered by LacZ staining of target cells. The maximum rescue corresponded to a titer of ~10⁵. Two independent experiments are presented. (F) Labeled virions imaged by confocal microscopy. Infectious viruses from a supernatant of 293 cells expressing both Gag-CFP (green) and Env-YFP (red) to label viral capsids and envelope, respectively, were bound to fibronectin-coated glass coverslips and imaged by confocal microscopy. Both colors exhibited a high degree of colocalization, suggesting that single particles are carrying both markers. (G) During viral entry, Env is released into the plasma membrane while Gag continues to move within the cytoplasm. Infectious two-colored MLV virions were generated carrying Env-YFP (red) and Gag-CFP (green) and added to DFJ8 cells. One hour after infection, the cells were fixed in 4% paraformaldehyde and imaged by confocal microscopy. A 0.4- μ m/step z-stack converted into a three dimensional (3-D) reconstruction is presented, viewed from the top of the cell. The white size bar corresponds to 5 μ m.

p12 of Gag has been altered to AAAA (Gag-PolAAAA) (26). The release of infectious virus produced by coexpression of plasmids encoding Gag-PolAAAA, Env and a viral RNA is reduced about 200-fold (data not shown). Coexpression of increasing amounts of Gag-CFP containing the wild-type PPPY motif resulted in a 33-fold rescue of infectious virus release (Figure 1E). This rescue was as efficient as for a wild-type Gag construct lacking both GFP and Pol (data not shown). 100% rescue did not occur because the enzymes encoded by Pol are diluted out in this experiment. A 100% replacement of Gag-PolAAAA by Gag-CFP results in a noninfectious virus lacking viral enzymes (Figure 1E). These experiments demonstrate that Gag-CFP can rescue

a budding defective virus *in trans*. Moreover, because the defective Gag-Pol must contribute the viral enzymes while Gag-CFP must recruit host factors required for virus budding, these experiments provide evidence that both Gag-

Pol and Gag-GFP are incorporated into the same particle, complementing the defects of the other. In contrast to the Gag-GFP fusion protein, which requires the coexpression of wild-type Gag-Pol, the Env-GFP fusion protein is tolerated



and gives rise to a replication competent MLV virus when inserted into full-length virus (Figure 1D). Cotransfection of Gag-CFP and Env-YFP together with plasmids encoding wild-type Gag-Pol and a viral RNA generated two-colored virions that were released into the cell supernatant containing both colors as determined by confocal microscopy (Figure 1F). When these two-colored virions were added to DF1 cells expressing MCAT-1, both colors separated, indicating membrane fusion and delivery of capsid into the cytoplasm (Figure 1G). While Env remained at the plasma membrane, capsids concentrated in a perinuclear region within the cytoplasm, consistent with the notion that these particles are on a functional route of entry. Because Gag- and Env-GFP fusion proteins were successfully incorporated into infectious particles, we were encouraged to utilize these constructs in order to monitor viral assembly and budding in the cells in which the fluorescent viruses were produced.

Gag localizes to late endosomal compartments

To visually assess the live dynamics of retroviral budding, we expressed MLV Gag-GFP proteins in 293 cells under our established conditions of infectious particle production: coexpressing a four-fold excess of wild-type Gag-Pol over Gag-CFP with a viral RNA and wild-type MLV Env. Examining confocal sections 24 h after transfection, we observed Gag-CFP localization to the surface of the cell, in particular at the cell-plate junction (Figure 2A), consistent with earlier studies using HIV Gag-GFP (23,24). Surprisingly, we also detected large amounts of Gag fluorescence in the interior of the cell, an unexpected result because MLV is a C-type retrovirus believed to assemble exclusively at the plasma membrane (Figure 2B,C) (3,27,28). Using time-lapse microscopy we noticed that dots of Gag fluorescence were consistently restricted to regions devoid of cytoplasm, suggesting that particles were moving within cytoplasmic vesicles (Figure 2D and supplemental movie for Figure 2D, movies available in the video gallery at <http://www.traffic.dk>). These vesicles were often considerably swollen, an effect that could be accentuated by increased Gag expression levels (data not shown). A similar distribution of Gag-GFP to the plasma membrane and to intracellular vesicles was observed when Gag-GFP was expressed in the absence of wild-type Gag-Pol and other viral components (data not shown), consistent with the ability of Gag alone to traffic to assembly sites and drive the release of virus-like particles (3,10,29). As such, a number of the following experiments were performed expressing Gag-GFP proteins in the absence of additional viral components.

We were interested in comparing the behavior of MLV Gag to that of HIV Gag. When HIV Gag-GFP (23) was expressed in 293 cells, we observed a distribution of Gag to both the plasma membrane and intracellular vesicles, similar to that seen for MLV Gag (Figure 2E, for entire Z-stack see supplemental movie for Figure 2E, movies available in the

video gallery at www.traffic.dk). To directly compare MLV and HIV Gag, we coexpressed MLV Gag-CFP and HIV Gag-YFP within the same cell (Figure 2F). Interestingly, although both Gag proteins localized to the plasma membrane as well as swollen intracellular vesicles, there was a marked preference of MLV Gag for internal membranes as compared to HIV Gag. Also, both Gag proteins localized to domains that largely excluded the other, suggesting homo-oligomerization in distinct regions at membranes.

To identify the nature of Gag⁺ intracellular membranes, we performed colocalization experiments using a variety of cellular markers. Our goal was to establish a fully visual system to study retroviral replication in living cells. As such, we accumulated a wide array of cellular GFP-fusion proteins to serve as markers for various cellular compartments (Table 1), many of which have been previously described to reflect the cell biology of the endogenous protein. For each marker, we determined the minimum amount of DNA, in the presence of excess carrier DNA that is required by transient transfection to visualize each cellular compartment. For example, transfection of a 35-mm dish of 293 cells with as little as 5 ng of Lamp1-YFP in a background of 1 μ g carrier DNA was sufficient to visualize the late endosomal/lysosomal compartment. Significant colocalization of either MLV or HIV Gag-CFP was found with the late endosomal markers rab7 and Lamp1 (Figure 3A,B for MLV, Figure 3F for HIV). Little to no colocalization was observed with the early endosomal markers rab5 or the PX domain of p40^{phox} (Figure 3C). No colocalization was observed with markers for either the recycling endosome (rab11) or the *trans*-Golgi (TGN38) (Figure 3D,E), indicating that Gag was not randomly associated with intracellular membranes, but specifically targeted to late endosomal vesicles. These results were verified in the absence of GFP-fusion proteins by immunofluorescence using antibodies against the endogenous proteins Lamp1, giantin and EEA1 (Supplemental Figure 1A,B available at http://www.traffic.dk/suppmat/4_11.asp and data not shown). In addition, Gag derived from replication competent MLV also localized to late endosomes in chronically infected cells (Supplemental Figure 1D,E). Gag localization to late endosomes was consistently observed in a variety of cell types including primary mouse embryonic fibroblasts (Supplemental Figure 1C–E).

Lamp1-positive vesicles containing Gag-CFP were highly motile, moving along in tubular structures at speeds up to 1.5 μ m/s (see supplemental movies a and b for Figure 3, movies available in the video gallery at www.traffic.dk). In addition to the classical perinuclear localization of late endosomes, a significant population of Lamp1 and Gag-positive vesicles localized to the periphery of the cell, in particular to cell protrusions (supplemental movie b for Figure 3). Interestingly, a number of Gag-CFP particles that appeared to localize to the surface of the cell were actually found to represent peripheral Lamp1-positive vesicles containing Gag-CFP fluorescence (Figure 3G,H).

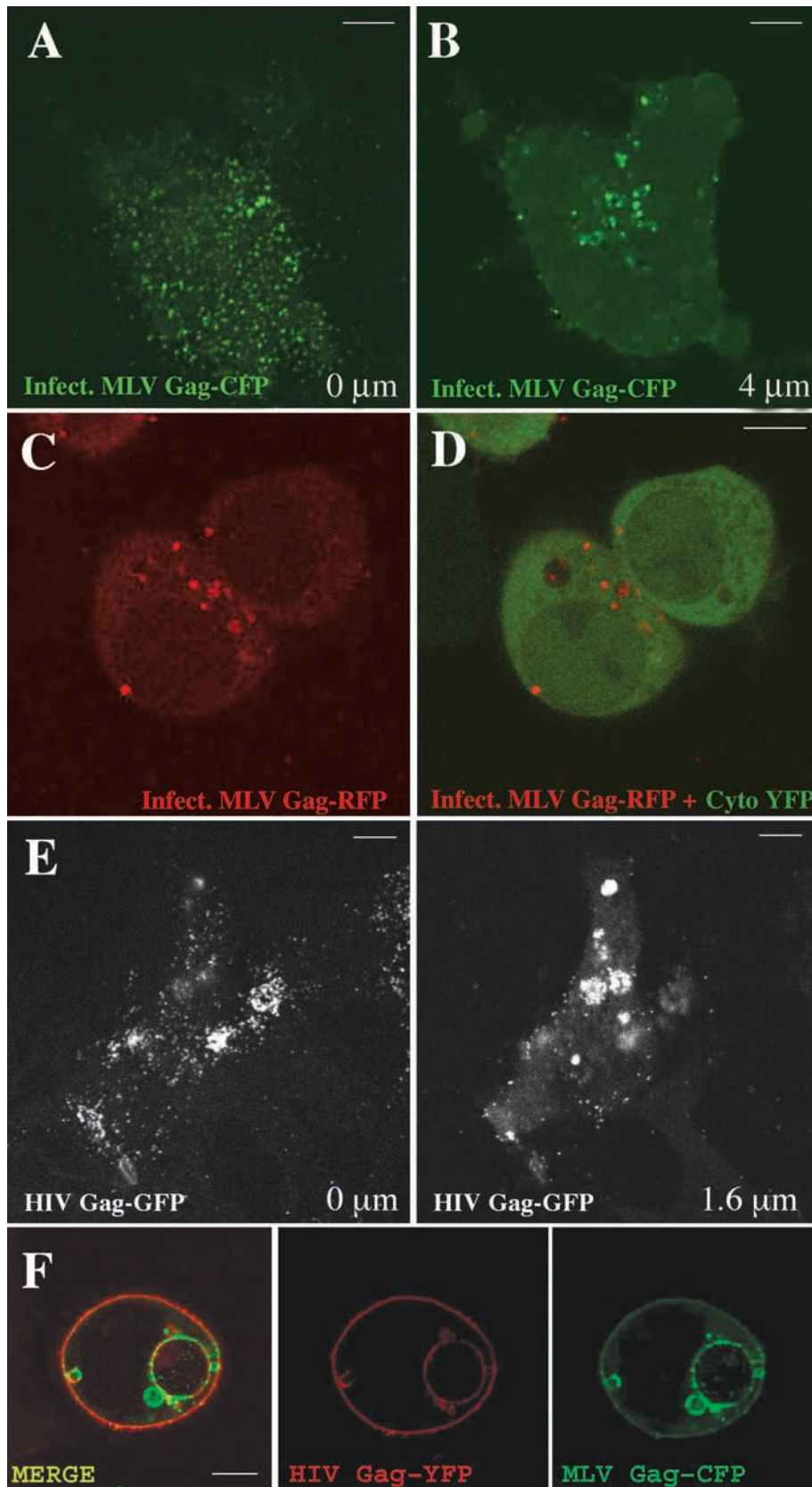


Figure 2: Intracellular localization of Gag-GFP fluorescence.

(A,B) MLV Gag-CFP was expressed in 293 cells under conditions of infectious particle production in order to image assembly and budding. The cells were fixed and analyzed by confocal microscopy at 30 h post transfection. Two Z-sections are presented, one showing the plasma membrane at the cell/plate junction (A) and another 4 μm above, showing the center of the cell (B). (C,D) Gag localizes to vesicles. Expression of MLV Gag-RFP (red), as in (A), was performed in the presence of a cytoplasmically expressed YFP (green) and imaged in living cells. Red (C) and red/green (D) channels are presented. (E) HIV Gag-GFP alone was expressed in 293 cells and imaged as in (A). The cell/plate junction (left panel) and a section of the center of the cell (right panel) are shown. (F) MLV Gag-CFP (green) and HIV Gag-YFP (red) were coexpressed in 293 cells and imaged by confocal microscopy. All size bars correspond to 5 μm .

Table 1: GFP-tagged cellular markers used in this study

	Marker	Reference
Golgi	TGN38-GFP	(56)
Early endosomes	GFP-Rab4	(55)
	GFP-Rab5	(55)
	PX ^{p40phox} -GFP	(54)
Recycling endosomes	GFP-Rab11	(55)
Late endosomes	GFP-Rab7	(52)
Lysosomes	Lamp1-GFP	(51)
Tetraspannins	GFP-CD63	(53)
	GFP-CD82	*
Vps machinery	Tsg101-GFP	*

* This paper.

A nearly 100% colocalization of MLV and HIV Gag was observed with the intracellular pools of CD63 or CD82, proteins of the tetraspannin family (Figure 3I,J). These proteins are signaling molecules that localize to the plasma membrane as well as intracellularly to exosomes, small vesicles that accumulate within MVBs (30). Swollen vesicles were observed containing Gag and either CD63 or CD82 GFP-fusion proteins within their interiors, suggesting that viruses and exosomes accumulate within MVBs.

Gag actively buds into late endosomes/multivesicular vesicles

An association of retroviral Gag proteins with late endosomal compartments could most easily be explained by endocytic reuptake of already released fluorescent viral

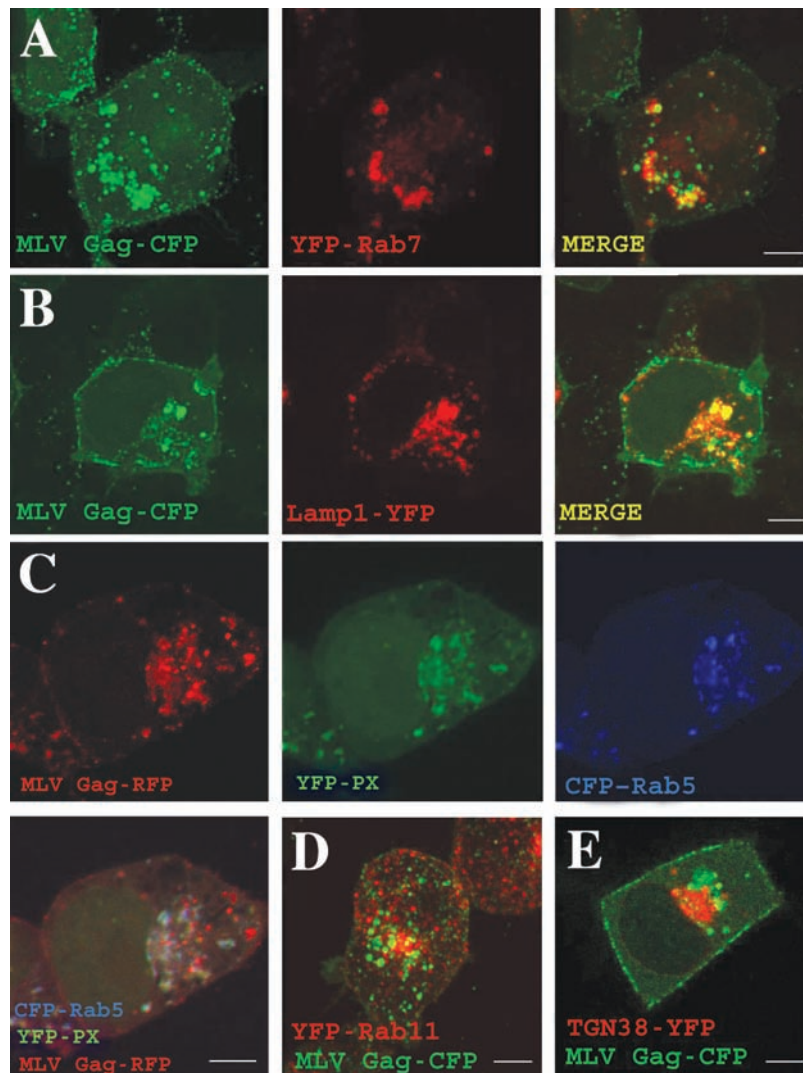


Figure 3: Gag localizes to late endosomal compartments. MLV Gag-GFP variants or HIV Gag-CFP were coexpressed in 293 (A–E, G–J) or HeLa cells (F) with the indicated cellular markers tagged with CFP or YFP. Cells were fixed at 30h post transfection and imaged in multitrack mode using the LSM 510 prior to pseudo-coloring as shown. Panels D and F represent 3-D reconstructions of 0.4 μm/step z-stacks. Panels G and H are z-slices taken 0.2 μm above the cell/plate junction. White arrows indicate peripheral Lamp1⁺ vesicles carrying Gag. All other images present z-sections taken through the center of the cell. Size bars correspond to 5 μm.

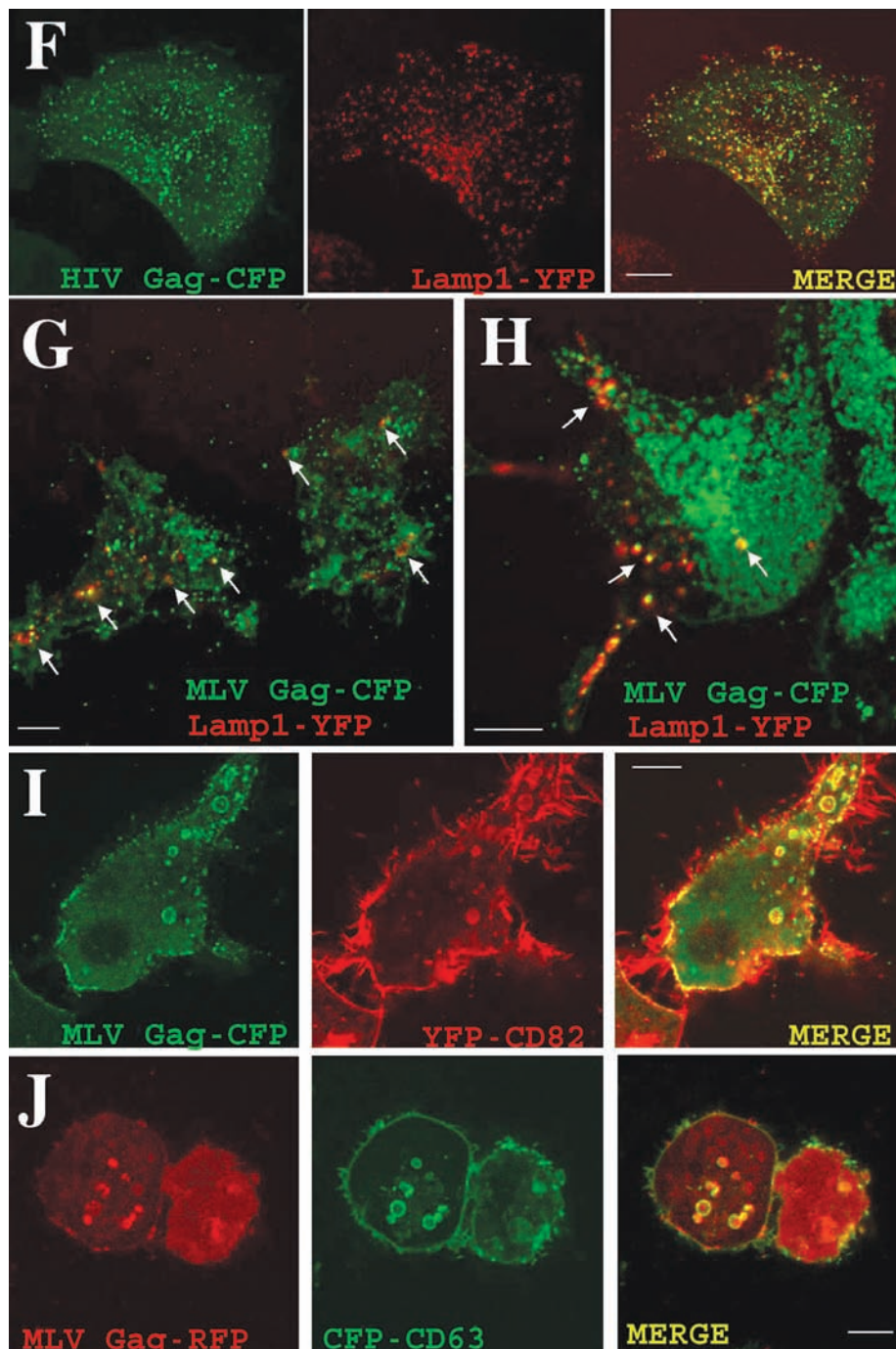


Figure 3: Continued

particles. Alternatively, given the recently defined role of the vacuolar protein sorting machinery in virus budding, Gag could potentially mimic cellular cargo destined for budding into MVBs.

If this notion were correct, we would expect to observe Gag binding to the cytoplasmic face of late endosomal vesicles and to detect budding intermediates forming

at the limiting membrane of MVBs. Indeed, we had repeatedly observed Gag fluorescence accumulating in specific patches on intracellular vesicles (Figure 4A–C). To facilitate imaging of the predominantly small endosomal vesicles, we took advantage of the ability of over-expressed Lamp1-YFP to aggregate lysosomal vesicles into larger assemblies to allow us to more easily monitor Gag assembly. These vesicles acquired rhodamine dextran, indicating

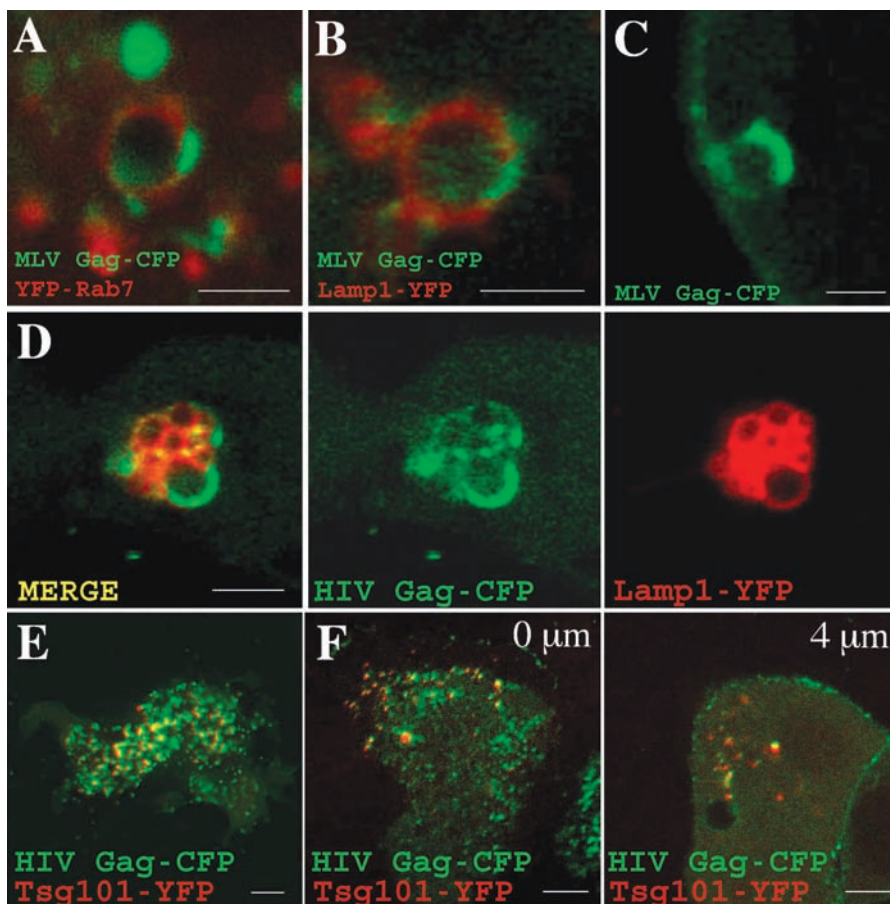


Figure 4: MLV and HIV Gag-GFP accumulate on the limiting membrane of late endosomal vesicles.

(A, B, C) Individual patches of MLV Gag-CFP (green) observed on Rab7⁺ or Lamp1⁺ intracellular vesicles in coexpression experiments as described in Figure 3. (D) Coexpression of HIV Gag-CFP with 50 ng Lamp1-YFP leading to large Lamp1⁺ vesicle assemblies. Size bars correspond to 1 μ m for (A–D). (E, F) HIV Gag-CFP colocalizes with Tsg101-YFP at both surface and intracellular sites, as imaged by confocal z-sectioning. (E) Colocalization at the cell/plate junction (0 μ m). (F) Colocalization at both the cell/plate junction (0 μ m) and at intracellular vesicles (4 μ m) within the same cell. Size bars correspond to 5 μ m for (E, F).

that they were functionally endosomal despite their aggregation (data not shown). When Gag was coexpressed under these conditions, we found Gag to accumulate in a bright rim at the cytoplasmic face of a subset of Lamp1-positive vesicles and to undergo Brownian motion within the lumen of these vesicles (Figure 4D; supplemental movies a,b for Figure 4D, movies available in the video gallery at www.traffic.dk). This phenotype cannot easily be explained by endocytic reuptake of released particles, but rather suggests that Gag can be targeted directly from the cytoplasm to endosomal membranes for budding. Interestingly, intense Gag binding appeared to compete Lamp1 away from the limiting membrane (Figure 4D).

Because the limited resolution of confocal microscopy does not allow conclusions regarding membrane topology, we performed transmission electron microscopy on double immunogold-labeled cryosections of 293 and HeLa cells expressing MLV and HIV Gag-GFP proteins in the absence of Lamp1-YFP expression (Figure 5). Electron micrographs confirmed the Gag coat observed by fluorescence microscopy as an electron-dense protein coat covering the cytoplasmic face of Lamp1-containing vesicles (Figure 5A, B for MLV, Figure 6A for HIV). The Gag coat was generally found on membranes exhibiting a tubular morphology (Figure 5A for MLV, Figure 6A for HIV) and

less often on spherical compartments (Figure 5B). The tubular morphology, as well as the relatively low amount of staining for Lamp1, suggests that these vesicles represent ‘earlier’ late endosomes active in membrane sorting. In addition to these tubular vesicles, more rounded vesicles were also observed that were completely filled with viral particles and had higher levels of Lamp1 staining (Figure 5A). These latter vesicles likely represent mature MVBs that store large numbers of viral particles. They were distinct from degradative lysosomes that contained few if any viral particles and large amounts of Lamp1 (data not shown). After investigating the population of tubular endosomes in more detail, we observed that Gag appeared to induce membrane bending (Figure 5C). Individual budding intermediates were identified, confirming active viral budding from Lamp1-positive limiting MVB membranes (Figure 5D for MLV, Figure 6B for HIV).

Consistent with our evidence for active budding both at the surface and at intracellular membranes in these cell types, Tsg101-YFP, a vps factor that binds to HIV Gag and is required for HIV budding (10), colocalized with HIV Gag-CFP both at the plasma membrane and at intracellular vesicles (Figure 4E, F). Taken together, these experiments provide evidence that retroviral Gag proteins can bud into late endosomal vesicles in 293 and HeLa cells.

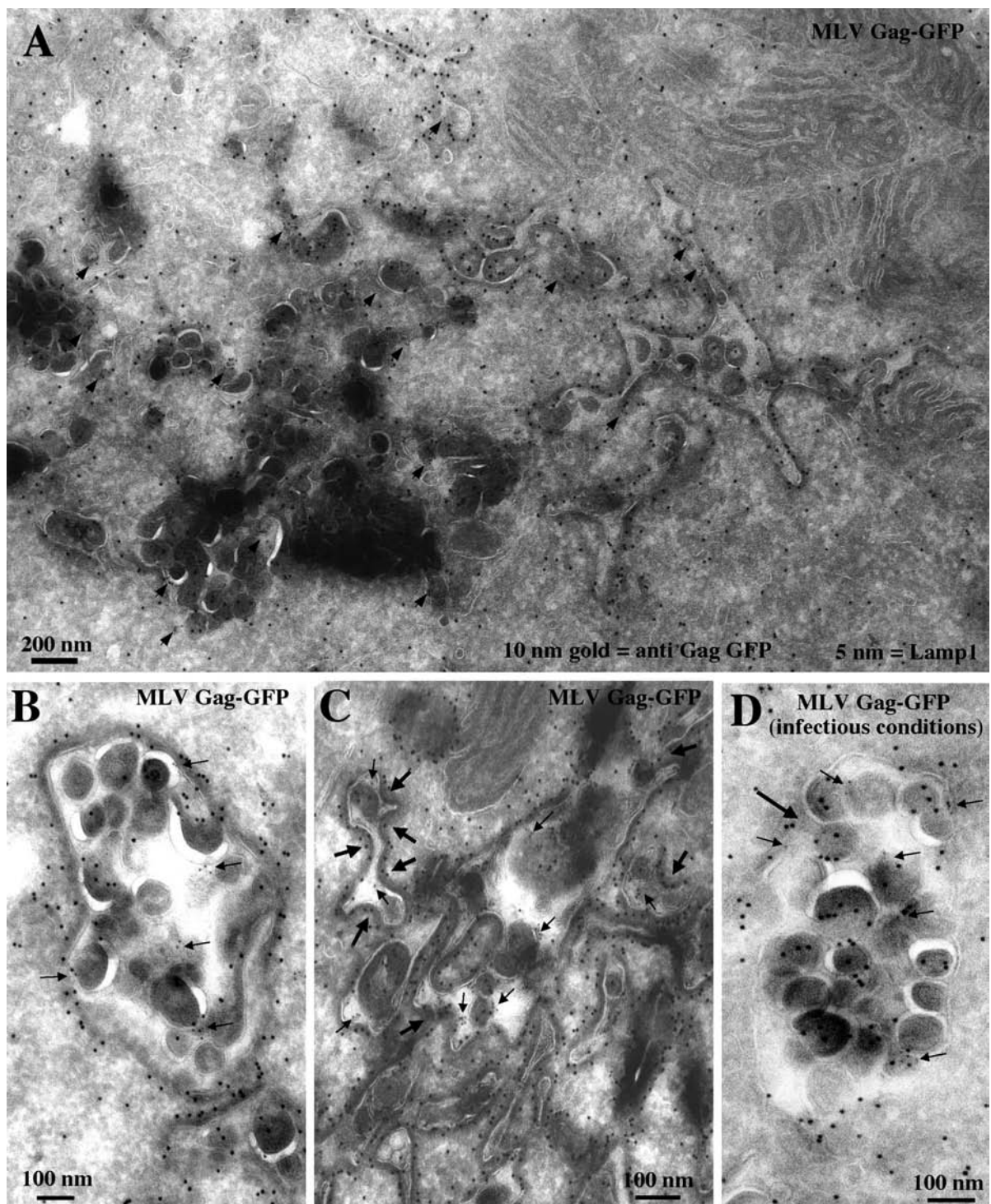


Figure 5: MLV budding into late endosomal vesicles. (A) Transmission electron microscopy of double immunogold labeled cryosections from 293 cells expressing MLV Gag-GFP. An anti-GFP antibody conjugated to 10 nm gold was used to identify Gag, and 5 nm gold was used to label endogenous Lamp1 (small arrows). Gag-GFP forms an electron-dense coat at the cytoplasmic face of tubular endosomal vesicles. In addition, more round vesicles lacking a Gag coat are observed that are completely filled with virus-like particles. As indicated by the micrograph, MLV Gag-GFP is found at a higher level in the cytoplasm as compared to HIV Gag-GFP (see Figure 6A). (B) An experiment as in (A) showing Gag-GFP forming a dense coat on a spherical multivesicular compartment full of virus-like particles. (C) Gag-induced bending (thick arrows) on Lamp1⁺ membranes (small arrows). (D) An electron micrograph showing an MLV budding site (thick arrow) on an endosomal compartment. Experiment as in (A), except that here all viral components were coexpressed under conditions of infectious virus production. Note that Lamp1 (small arrows) is found on both the limiting membrane as well as the envelope of budded virions.

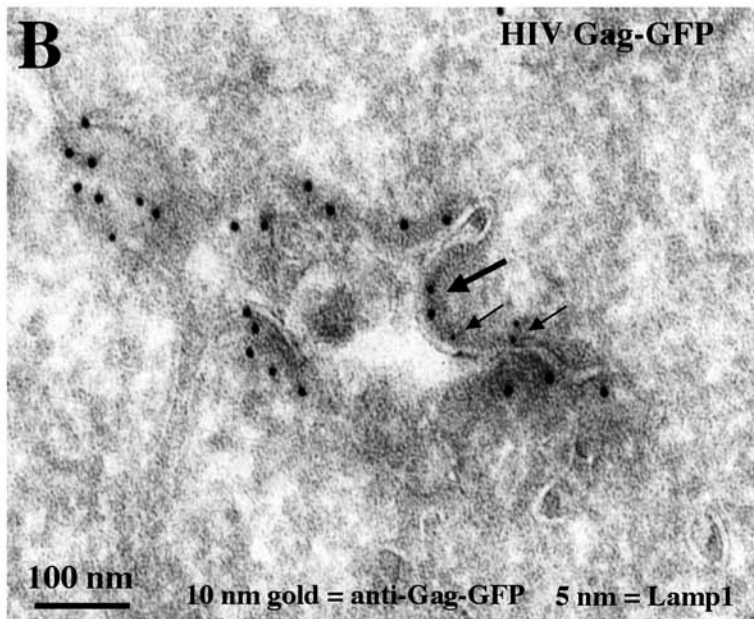
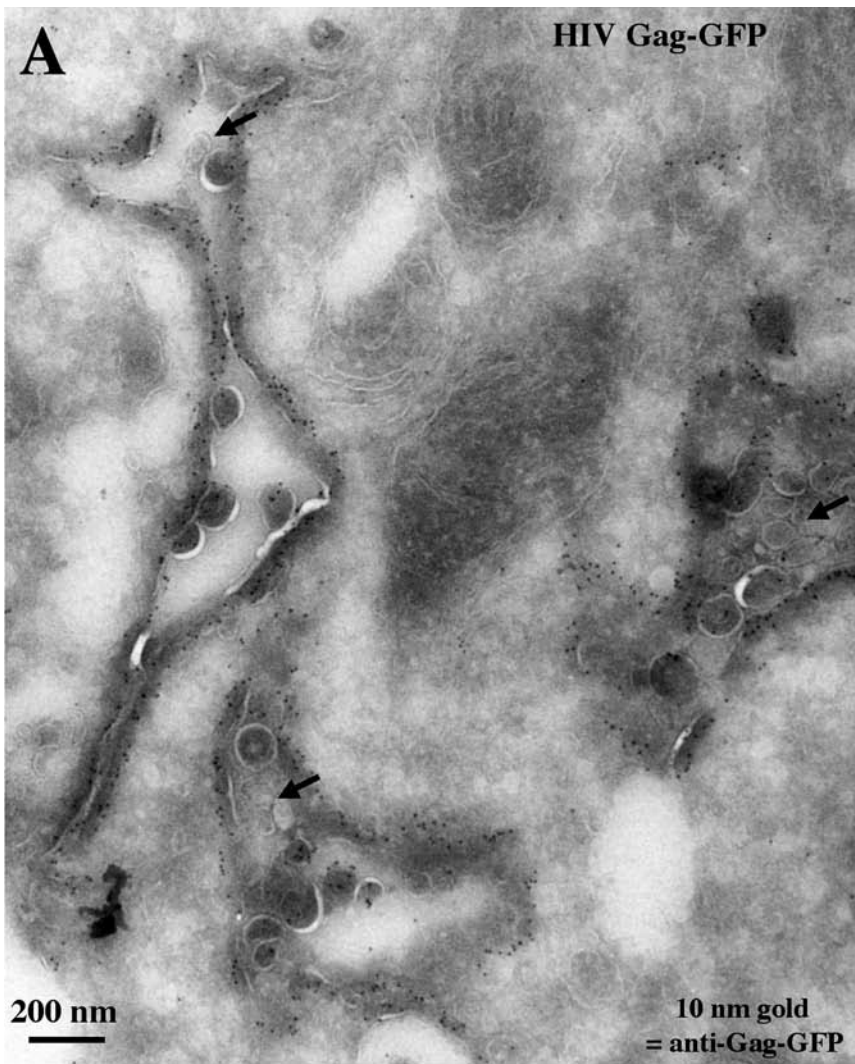


Figure 6: HIV Gag budding into late endosomal vesicles in HeLa cells. (A) Transmission electron micrograph of HIV Gag-GFP forming an electron-dense coat on intracellular membranes containing small exosomes (thick arrows) in addition to electron-dense and gold-labeled virus-like particles. (B) Micrograph as in (A) showing HIV Gag-GFP assembling into a virus-like particle (thick arrow) at Lamp1⁺ membranes (small arrows).

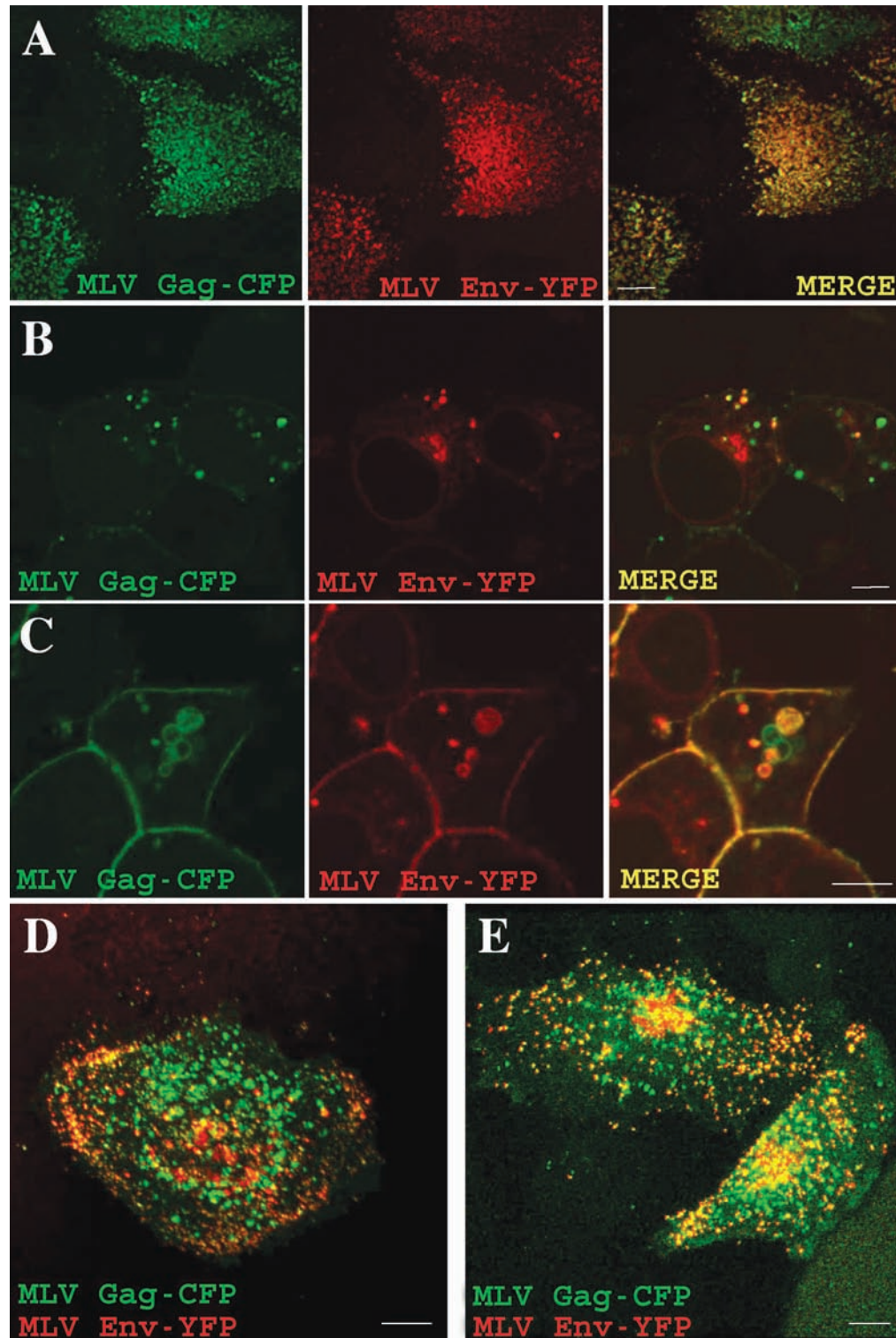


Figure 7: Env colocalizes with Gag at the cell surface as well as at intracellular vesicles. (A) MLV Gag-CFP (green) and Env-YFP (red) were coexpressed in 293 cells and plasma membrane fluorescence was imaged by confocal analysis of the cell/plate junction. (B–E) Experiments as in (A), showing additional colocalization of Gag-CFP and Env-YFP to a subset of intracellular compartments. (D) and (E) represent 3-D reconstructions of z-stacks of transfected HeLa cells. Gag-CFP and Env-YFP were coexpressed in the absence of other viral factors in (C) and (D). (A) (B) and (E) represent conditions of infectious particle production. Size bars correspond to 5 μm.

MLV envelope colocalizes to a subset of intracellular vesicles

The formation of infectious retroviral particles requires the co-recruitment of retroviral envelope proteins (Env) into the viral membrane during budding. To monitor Env and Gag assembly simultaneously, we coexpressed MLV Env-YFP with MLVGag-CFP under conditions of infectious virus production. Under these conditions, all fluorescent dots detected at the plasma membrane were two-colored, representing the colocalization of Env-YFP with Gag-CFP (Figure 7A). Confocal cytoplasmic sections of cells revealed a similar colocalization of Env-YFP with Gag-CFP at intracellular vesicles (Figure 7B), including within the interior of large MVBs (Figure 7C). Interestingly, a number of perinuclear Gag-positive vesicles lacked Env-YFP fluorescence. In general, the more peripheral Gag-positive vesicles were more likely to also contain Env-YFP (Figure 7B,D,E).

Net movement of MLV Gag-GFP from intracellular membranes to the surface correlates with infectious virus release

The association of Gag and Env with intracellular membranes in 293 and HeLa cells could represent trafficking within the degradative pathway. Alternatively, Gag association with endosomal membranes may be contributing to viral egress. The rapid movement of Gag positive vesicles within the cytoplasm made it difficult to track individual particles over time. To gain insight into the process of virus production by transient expression in 293 cells, we quantified the distribution of MLV Gag-CFP between intracellular membranes and the cell surface and compared it with the release of infectious virus from cells over a time-course of 54 h (Figure 8). These experiments revealed a net movement of MLV Gag from intracellular membranes to the cell surface over time, which correlated well with an increase

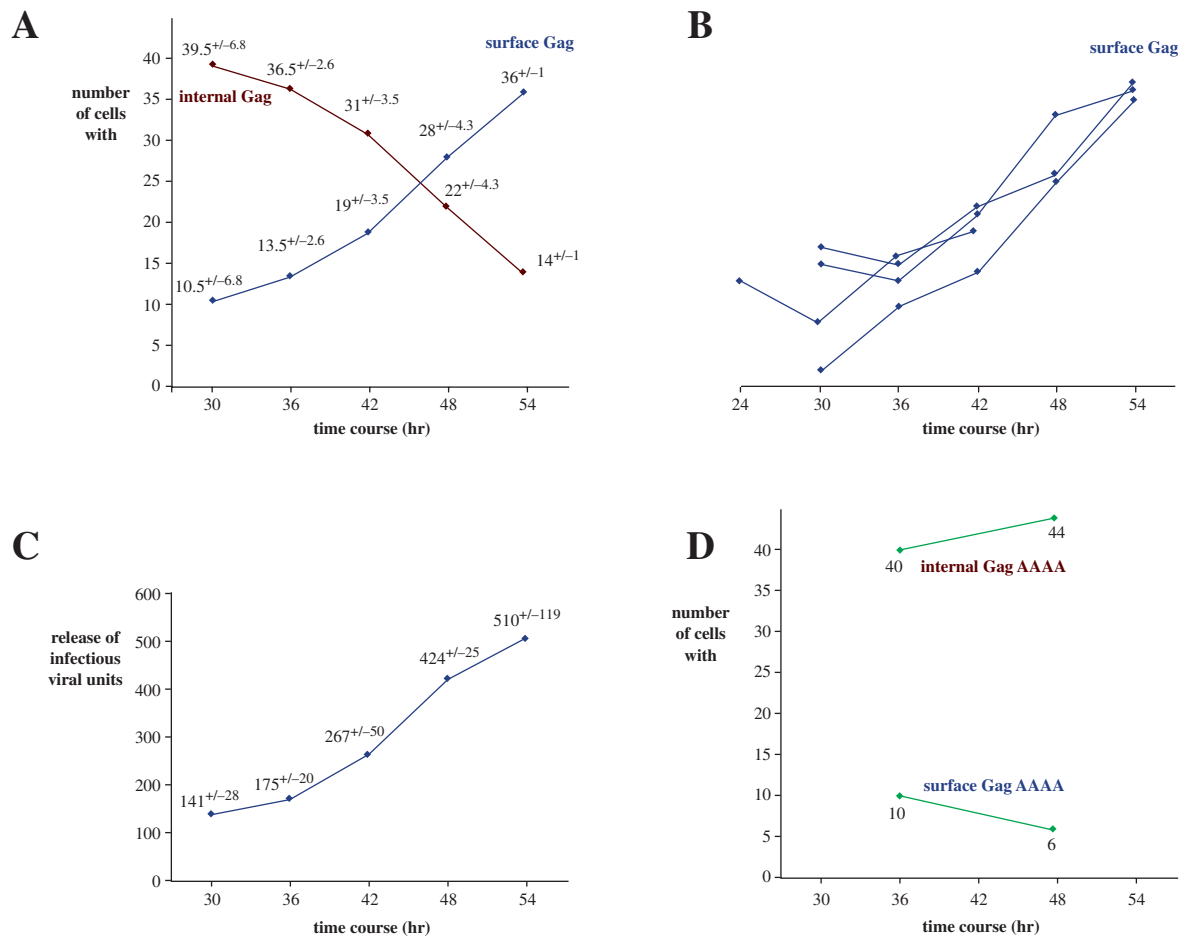


Figure 8: MLV Gag-CFP localization shifts from intracellular membranes to the surface over time. (A–C) 293 cells were transfected with Gag-CFP with or without conditions of infectious virus production. Every 6 h, the cell supernatants were harvested, filtered and titered for LacZ expression on DFJ8 cells. Average values with STDEV for 3 independent experiments are presented in (C). For each time-point, z-stacks (1 μm/step) were acquired for 50 producer cells by confocal microscopy, resulting in stacks of ~18 slices/cell. Cells were scored for significant Gag-CFP particles within the cytoplasm vs. cells that only exhibited Gag-CFP fluorescence at the plasma membrane. A standard image was aligned next to all analyzed z-slices to control for bias. The graph shown in (A) presents the average number of cells (out of 50) for either surface or internal Gag-CFP fluorescence from 4 individual experiments depicted in (B). (D) The experiment was repeated for two time-points following the localization of budding defective Gag-CFP carrying a mutated PPPY (Gag AAAA).

in the release of infectious particles (compare Figure 8A,B with 8C). An MLVGag-CFP mutant that is impaired in budding failed to go through this transition (Figure 8D). These results argue against an endocytic reuptake of released virions as an explanation for the association of Gag and Env with late endosomal membranes. In fact, particles did not accumulate within cells despite a concurrent accumulation of released particles at the surface of the cell. Rather, these data suggest that Gag associated with late endosomal membranes at early time points is on a functional route directed towards the plasma membrane.

Discussion

Using a novel visual system we have identified multivesicular bodies (MVBs) as intracellular assembly and budding sites for MLV and HIV Gag in 293 and HeLa cells that were previously believed to only support budding at the plasma membrane (3,23). MLV and HIV Gag were specifically targeted to the cytoplasmic face of late endosomal membranes where virus-like particles or mature virions were detected budding into the lumen of the vesicle. Env joined Gag in a largely peripheral subpopulation of MVBs. These experiments indicate that Gag association with endosomal membranes and subsequent budding into MVBs is not restricted to macrophages but exists as a constitutive pathway in multiple cell types. Thus, retroviruses can interact with the vacuolar protein sorting machinery in a more traditional sense, directly linked to the mechanism by which cellular proteins are sorted into multivesicular bodies. Moreover, the observed movement of Gag from intracellular sites to the surface over time suggests that Gag-induced membrane trafficking contributes to viral egress even in cells where budding occurs predominantly at the surface. The mechanisms of surface and MVB budding may not necessarily be mutually exclusive. Gag targeting to endosomal membranes may promote tubular membrane sorting of the vps machinery to the plasma membrane for surface budding, as suggested for Marburg virus (31), while also redirecting MVBs to fuse with the plasma membrane in order to release stored virions. Interestingly, Gag lacking the late domain motif PPPY fails to promote movement of Gag towards the surface. This observation implies that budding motifs within Gag also recruit cellular factors that are involved in the sorting of endosomal membranes to the plasma membrane.

How Gag is targeted to MVBs is unknown. It is possible that Gag is first trafficked to the plasma membrane, or even to the Golgi where it would be ubiquitinated for sorting into MVBs. In this sense, Gag may mimic unfolded proteins destined for sorting into MVBs, but subsequently escape the cellular garbage pathway by directing MVB movement to the surface. This pathway could resemble the sorting of yeast carboxypeptidase S and polyphosphatase

phosphatase to the yeast vacuole. These proteins also likely mimic unfolded cellular proteins in order to be sorted into the MVB where they perform their enzymatic functions (32).

Consistent with our observations, two additional models of viral budding and egress cannot be ruled out. First, there is evidence that Gag is able to recruit the purely cytosolic vps complexes (11) to budding sites without altering membrane sorting events (8). For instance, it remains to be resolved how mutations within HIV matrix can redirect budding into the endoplasmic reticulum (33). Second, we have repeatedly observed the formation of gigantic vacuoles filled with thousands of Gag-GFP fluorescent particles (Supplemental Figure 2A,B available at http://www.traffic.dk/suppmat/4_11.asp/ and movies a,b, movies available in the video gallery at www.traffic.dk). These vesicles can fuse with the plasma membrane to release virions (Supplemental Figure 2C). The large volume of these compartments raises the possibility of a lytic contribution to virus release, especially for highly cytopathic viruses.

Our observation of tubular membrane sorting events, as well as the notion of the likely release of viruses via MVB fusion with the surface of the cell resembles the controversy surrounding MHC class II presentation in dendritic cells. Strong evidence has recently been presented for the fusion of exosomes carrying class II molecules to the limiting membrane of the MHC class II compartment, followed by trafficking via tubules to the plasma membrane (34–36). Alternatively, the release of exosomes bearing class II molecules has also been documented (37,38). These similarities to retroviral behavior are reinforced by the observation that Gag expression can rescue the delivery of HLA-DR from the MHC class II compartment to the surface in a mutant cell line (39). It is intriguing to speculate that viruses evade the immune system by utilizing the antigen presentation pathway for the purpose of viral spread.

While it remains unclear to what extent budding into MVBs contributes functionally to virus release in 293 and HeLa cells, the mobilization and fusion of MVBs with the plasma membrane has been well documented in B cells, dendritic cells, and macrophages (22,40); antigen-presenting cells in which many retroviruses initially replicate before spreading to T cells during the later stages of infection (41,42). It may be advantageous for these viruses to initially utilize intracellular vesicles as a safe haven for virus assembly in the face of an active immune response, as proposed in the 1980's by Gendelman and colleagues (19,43). Viruses would bud internally into MVBs and later be mobilized to fuse with the plasma membrane by signaling events initiated by cell–cell contact. Virus transmission could then occur in shielded contact zones in an environment inaccessible to antibody recognition. Once the immune system weakens, virus production could predominate in T cells, where budding appears to take place at the cell surface.

In view of a general MVB budding pathway, the presentation of HIV to T cells by dendritic cells may present a variation on this theme. Dendritic cells that cannot be infected by HIV internalize the virus via interactions with DC-SIGN into an acidic endosomal compartment (44,45). Interactions with T cells could lead to mobilization of these vesicles and their release at the cell–cell contact zone (46). Thus, MVB trafficking may represent a general pathway for viral transmission to T cells from infected macrophages and B cells as well as for uninfected dendritic cells harboring virus.

While this manuscript was under review, Pelchen-Matthews, Kramer and Marsh published a detailed analysis of HIV budding into MVBs in primary human macrophages (47). The data have striking similarities to those presented in this manuscript. Both works demonstrate retroviral budding from the limiting membrane of a largely tubular compartment surrounded by an electron-dense protein coat. Virus or virus-like particles accumulate in MVBs positive for CD63, CD82 and relatively small amounts of Lamp1. The work by Pelchen-Matthews and colleagues elegantly demonstrates that HIV virions generated intracellularly by budding into endosomal membranes are released from macrophages. Our work suggests that Gag proteins of at least two retroviruses possess intrinsic cell biological properties providing for the association with and budding into endosome-derived membranes in a variety of cell types. Future work will determine the functional significance and mechanistic details of this interplay between Gag and the endosomal systems of varying cell types.

Materials and Methods

Plasmids

HIV Gag-CFP or -YFP was generated by insertion of the EcoRI-BamHI fragment of pGag-GFP (Marilyn Resh & George Pavlakis, National Cancer Institute-Frederick, MD, USA) (23) into pECFP-N1 or pEYFP-N1 (Clontech, Palo Alto, CA, USA). MLV Gag-CFP, a CFP-fusion to the amino acids PQ at the C-terminus of the Gag NC domain, was cloned by replacing Pol with CFP in pMDoldGag-Pol (Richard Mulligan, Harvard Medical School, Boston, MA, USA). To prepare MLV Gag-RFP, the MLV Gag ORF was inserted into the BamHI-AgeI sites of a generated pmRFP-N1. mRFP was a kind gift of Roger Tsien (University of California-San Diego, San Diego, CA, USA) (48). MLV Gag-CFPAAAA and Gag-PolAAAA were prepared by site-directed mutagenesis. Friend MLV Env-YFP was generated by YFP insertion into the NheI site of the construct pFr-MuLV273/274 (49) and transfer of the Env gene into pcDNA3. MCAT-CFP was a variant of MCAT-GFP (50). Lamp1-YFP was created by insertion of the Lamp1-coding region of pLamp1-GFP (Norma Andrews, Yale University, New Haven, CT, USA) (51) into the EcoRI-BamHI sites of pEYFP-N1 (Clontech, Palo Alto, CA, USA). YFP-Rab7 was

generated through transfer of the Rab7-coding region of pGL-GFP-Rab7 (Craig Roy, Yale University, New Haven, CT, USA) (52) into the XhoI-HindIII sites of pEYFP-C1 (Clontech, Palo Alto, CA, USA). CFP/YFP-CD63 and YFP-CD82 were created by insertion of the coding regions from pBosEGFP-CD63 (Gillian Griffiths, Oxford University, Oxford, UK) (53) and p2.1 CD82 (Peter Cresswell, Yale University, New Haven, CT, USA), respectively, into the XhoI-HindIII sites of pEYFP-C1 (Clontech, Palo Alto, CA, USA). p40PX-EYFP was a gift of Michael Yaffe (Massachusetts Institute of Technology, Boston, MA, USA) (54). PH-Akt-YFP was a gift of Johannes Huppa (Stanford University, Palo Alto, CA, USA). YFP-Rab4, YFP-Rab5, and YFP-Rab11 were gifts of Marino Zerial (Max Planck Institute, Dresden, Germany) (55). TGN38-YFP was cloned by insertion of the TGN38-coding region of TGN38-GFP (George Banting, University of Bristol, Bristol, UK) (56) into XhoI-BamHI sites of pEYFP-N1. Tsg101-YFP was cloned by insertion of the Tsg101 ORF from pIRES-Tsg101 (Wes Sundquist, University of Utah, Salt Lake City, UT, USA) (10) into XhoI-HindIII of pEYFP-N1.

Production of fluorescent MLV virions

To produce Env-YFP-labeled MLV virions, YFP was cloned into the NheI site of the Friend 57–273/4 construct from Abraham Pinter (New York University, New York, NY, USA) (49). This construct generates a replication-competent virus, which was produced in a chicken cells stably expressing MCAT-1 (DFJ8 cells; Stephen Hughes, National Cancer Institute-Frederick, Frederick, MD, USA) (57). Supernatants from roller bottle cultures were filtered (0.45 μm), concentrated by ultracentrifugation through a 15% sucrose cushion, resuspended in media/10%FBS and filtered a second time (0.2 μm). 50- μl aliquots were stored at -80°C .

To produce two-colored virions in 293 cells, a 10-cm dish of 293 cells was transfected using 36 μl FuGene 6 (Roche, Indianapolis, IN, USA) in 1 ml serum-free media mixed with 4 μg of a plasmid encoding a viral RNA (pMMP-LTR-LacZ; Richard Mulligan, Harvard Medical School, Boston, MA, USA), 4 μg FrEnv-YFP (pCDNA3), 1 μg MLV Gag-CFP and 3 μg wild-type GagPol (pMDoldGag-Pol; Richard Mulligan, Harvard Medical School, Boston, MA, USA). The medium was changed at 20 h and cells were split into a 15-cm dish. At 48 h post transfection, the viral supernatant was harvested as described above.

Cell transfection or infection

293, HeLa, NRK and NIH 3T3 cells were maintained in DMEM high glucose (Invitrogen, Carlsbad, CA, USA) containing 10% FBS plus Pen/Strep/Glutamine. For imaging, cells were transfected overnight in 6-well plates using the following plasmid amounts per single 35-mm dish: HIV or MLV Gag-CFP: 200 ng^{-1} μg (293, NRK) or 1–2 μg (HeLa). MLVEnv-YFP or Tsg101-YFP: 200 ng (293) or 500 ng

(HeLa). CFP/YFP-CD63, YFP-CD82, YFP-Rab4 and YFP-Rab5: 50 ng (293, NRK), 200 ng (HeLa). p40PX-YFP: 40 ng (293). YFP-Rab7 and YFP-Rab11: 20 ng (293), 80 ng (HeLa). Lamp1-YFP or TGN38-YFP: 5 ng (293) or 50 ng (HeLa). All DNAs were brought up to 2 μ g total DNA using Herring Testes Carrier DNA (Invitrogen, Carlsbad, CA, USA) in 100 μ l serum-free media mixed with 6 μ l of FuGene 6 reagent (Roche, Indianapolis, IN, USA) for transfection. To image assembly and budding under conditions of infectious virus production, 35-mm dishes of 293 cells were transfected with 600 ng LTR LacZ, 100–600 ng wild-type Env or Env-YFP, 450 ng wild-type GagPol and 150 ng Gag-CFP/RFP (5.6 μ l FuGene 6 in 100 μ l serum-free media). Mouse embryonic fibroblasts (a gift of Ute Felbor, University of Wurzburg, Wurzburg, Germany) or mouse NIH 3T3 cells were infected with replication-competent Moloney MLV carrying a FLAG epitope tag within the p12 domain of Gag (generated from pNCS/Flag, Steve Goff, Columbia University, New York, NY, USA) (58).

Confocal imaging, immunofluorescence and electron microscopy

For live confocal imaging, cells were transferred 10–16 h post transfection to poly L-lysine coated 35-mm glass-bottom plates (MatTek, Ashland, MA, USA). At 24–48 h post transfection, medium was replaced with DMEM (10% FBS) supplemented with 10 mM HEPES pH 7.4, equilibrated to 5% CO₂, and covered with mineral oil (Roxane, Columbus, OH, USA) to prevent evaporation. Live imaging was carried out using the 100 \times objective of a Zeiss LSM510 Confocal Microscope equipped with Metadector (Zeiss, Jena, Germany). Alternatively, cells were transfected on or transferred post transfection to glass coverslips prior to fixation with 4% paraformaldehyde (PFA). For endosomal immunofluorescence, cells were PFA-fixed and permeabilized with saponin (Sigma, St. Louis, MO, USA) prior to incubation with either rat anti-mouse EEA1 (BD Biosciences, Palo Alto, CA, USA), mouse anti-human (H4A3) or rat anti-mouse (ID4B) Lamp1 antiserum (developed by J. Thomas August and James E.K. Hildreth and obtained from the Developmental Studies Hybridoma Bank (DSHB), Iowa City, IA, USA). For Giantin immunofluorescence, cells were fixed in MeOH at –20 °C before rehydration with PBS and incubation with mouse anti-giantin antiserum (Graham Warren, Yale University, New Haven, CT, USA). Rhodamine-conjugated secondary antisera were purchased from Jackson ImmunoResearch, Inc. (West Grove, PA, USA). Transmission electron microscopy of immunogold-labeled cryosections was performed as previously described (59,60). Immunolabeling of cryosections was performed using primary rabbit anti-GFP antibodies (Invitrogen, Carlsbad, CA, USA) and mouse anti-human or rat anti-mouse Lamp1 antibodies (H4A3 and ID4B, respectively). Gold labeling was performed either directly or after secondary labeling with rabbit anti-mouse or anti-rat antibodies, followed by protein A coupled

to either 5- or 10-nm gold particles (Utrecht University, the Netherlands).

Acknowledgments

We are grateful for the assistance of Kim Zichichi and Carolyn Marks from the electron microscopy facility at Yale. We thank all of our colleagues who provided us with valuable plasmids (see Material and Methods and Table 1 for the origins of all reagents). We thank Norma Andrews for critical reading of the manuscript and Jon Kagan for helpful discussions. This work was supported by the Hellman Family Fellowship, the Searle Scholars Program, the Yale Cancer Center and NIH grant 1R01CA098727-0 to W.M., as well as the NIH grants GM 57256-04 to P.A. and HL 07680 to G.C. M. L. is a Leopoldina Fellow and J.C. is a Howard Hughes Medical Institute Investigator.

References

- Gottlinger HG. The HIV-1 assembly machine. *Aids* 2001;15 (Suppl. 5): S13–S20.
- Goff S. Retroviridae: the retroviruses and their replication. In: Knipe DM, Howley PM, eds. *Fields Virology*, 4th edn. Philadelphia: PA: Lippincott; 2001. pp 1871–1940.
- Swanstrom R, Wills JW. Synthesis, assembly, and processing of viral proteins. In: Coffin JM, Hughes SH, Varmus HE, eds. *Retroviruses*. Cold Spring Harbor, N.Y.: Cold Spring Harbor Laboratory Press; 1997. pp 263–334.
- Sakalian M, Hunter E. Molecular events in the assembly of retrovirus particles. *Adv Exp Med Biol* 1998;440:329–339.
- Carter CA. Tsg101: HIV-1's ticket to ride. *Trends Microbiol* 2002;10:203–205.
- Freed EO. Viral late domains. *J Virol* 2002;76:4679–4687.
- Vogt VM. Ubiquitin in retrovirus assembly: actor or bystander? *Proc Natl Acad Sci USA* 2000;97:12945–12947.
- Pornillos O, Garrus JE, Sundquist WI. Mechanisms of enveloped RNA virus budding. *Trends Cell Biol* 2002;12:569–579.
- Gottlinger HG, Dorfman T, Sodroski JG, Haseltine WA. Effect of mutations affecting the p6 gag protein on human immunodeficiency virus particle release. *Proc Natl Acad Sci USA* 1991;88:3195–3199.
- Garrus JE, von Schwedler UK, Pornillos OW, Morham SG, Zavitz KH, Wang HE, Wettstein DA, Stray KM, Cote M, Rich RL, Myszka DG, Sundquist WI. Tsg101 and the vacuolar protein sorting pathway are essential for HIV-1 budding. *Cell* 2001;107:55–65.
- Katzmann DJ, Odorizzi G, Emr SD. Receptor downregulation and multivesicular-body sorting. *Nat Rev Mol Cell Biol* 2002;3:893–905.
- Katzmann DJ, Babst M, Emr SD. Ubiquitin-dependent sorting into the multivesicular body pathway requires the function of a conserved endosomal protein sorting complex, ESCRT-I. *Cell* 2001;106:145–155.
- Pornillos O, Alam SL, Davis DR, Sundquist WI. Structure of the Tsg101 UEV domain in complex with the PTAP motif of the HIV-1 p6 protein. *Nat Struct Biol* 2002;9:812–817.
- Harty RN, Brown ME, Wang G, Huibregtse J, Hayes FP. A PPxY motif within the VP40 protein of Ebola virus interacts physically and functionally with a ubiquitin ligase: implications for filovirus budding. *Proc Natl Acad Sci USA* 2000;97:13871–13876.
- Kikonyogo A, Bouamr F, Vana ML, Xiang Y, Aiyar A, Carter C, Leis J. Proteins related to the Nedd4 family of ubiquitin protein ligases interact with the L domain of Rous sarcoma virus and are required for gag budding from cells. *Proc Natl Acad Sci USA* 2001;98:11199–11204.

16. Strack B, Calistri A, Accola MA, Palu G, Gottlinger HG. A role for ubiquitin ligase recruitment in retrovirus release. *Proc Natl Acad Sci USA* 2000;97:13063–13068.
17. Patnaik A, Chau V, Wills JW. Ubiquitin is part of the retrovirus budding machinery. *Proc Natl Acad Sci USA* 2000;97:13069–13074.
18. Martin-Serrano J, Zang T, Bieniasz PD. HIV-1 and Ebola virus encode small peptide motifs that recruit Tsg101 to sites of particle assembly to facilitate egress. *Nat Med* 2001;7:1313–1319.
19. Orenstein JM, Meltzer MS, Phipps T, Gendelman HE. Cytoplasmic assembly and accumulation of human immunodeficiency virus types 1 and 2 in recombinant human colony-stimulating factor-1-treated human monocytes: an ultrastructural study. *J Virol* 1988;62:2578–2586.
20. Raposo G, Moore M, Innes D, Leijendekker R, Leigh-Brown A, Benaroch P, Geuze H. Human macrophages accumulate HIV-1 particles in MHC II compartments. *Traffic* 2002;3:718–729.
21. Mellman I, Steinman RM. Dendritic cells: specialized and regulated antigen processing machines. *Cell* 2001;106:255–258.
22. Thery C, Zitvogel L, Amigorena S. Exosomes. composition, biogenesis and function. *Nat Rev Immunol* 2002;2:569–579.
23. Hermida-Matsumoto L, Resh MD. Localization of human immunodeficiency virus type 1 Gag and Env at the plasma membrane by confocal imaging. *J Virol* 2000;74:8670–8679.
24. Sandefur S, Varthakavi V, Spearman P. The I domain is required for efficient plasma membrane binding of human immunodeficiency virus type 1 Pr55Gag. *J Virol* 1998;72:2723–2732.
25. Rosenberg N, Jolicoeur P. Retroviral pathogenesis. In: Coffin JM, Hughes SH, Varmus HE, eds. *Retroviruses*. Cold Spring Harbor, N.Y.: Cold Spring Harbor Laboratory Press; 1997. pp 475–586.
26. Yuan B, Li X, Goff SP. Mutations altering the Moloney murine leukemia virus p12 Gag protein affect virion production and early events of the virus life cycle. *EMBO J* 1999;18:4700–4710.
27. Hunter E. Virus assembly. In: Knipe DM, ed. *Fields Virology*. Philadelphia: Lippincott Williams&Wilkins; 2001. pp 171–198.
28. Sandefur S, Smith RM, Varthakavi V, Spearman P. Mapping and characterization of the N-terminal I domain of human immunodeficiency virus type 1 Pr55 (Gag). *J Virol* 2000;74:7238–7249.
29. Freed EO. HIV-1 gag proteins: diverse functions in the virus life cycle. *Virology* 1998;251:1–15.
30. Escola JM, Kleijmeer MJ, Stoorvogel W, Griffith JM, Yoshie O, Geuze HJ. Selective enrichment of tetraspan proteins on the internal vesicles of multivesicular endosomes and on exosomes secreted by human B-lymphocytes. *J Biol Chem* 1998;273:20121–20127.
31. Kolesnikova L, Bugany H, Klenk HD, Becker S. VP40, the matrix protein of Marburg virus, is associated with membranes of the late endosomal compartment. *J Virol* 2002;76:1825–1838.
32. Reggiori F, Pelham HR. A transmembrane ubiquitin ligase required to sort membrane proteins into multivesicular bodies. *Nat Cell Biol* 2002;4:117–123.
33. Facke M, Janetzko A, Shoeman RL, Krausslich HG. A large deletion in the matrix domain of the human immunodeficiency virus gag gene redirects virus particle assembly from the plasma membrane to the endoplasmic reticulum. *J Virol* 1993;67:4972–4980.
34. Kleijmeer M, Ramm G, Schuurhuis D, Griffith J, Rescigno M, Ricciardi-Castagnoli P, Rudensky AY, Ossendorp F, Melief CJ, Stoorvogel W, Geuze HJ. Reorganization of multivesicular bodies regulates MHC class II antigen presentation by dendritic cells. *J Cell Biol* 2001;155:53–63.
35. Chow A, Toomre D, Garrett W, Mellman I. Dendritic cell maturation triggers retrograde MHC class II transport from lysosomes to the plasma membrane. *Nature* 2002;418:988–994.
36. Boes M, Cerny J, Massol R, Op den Brouw M, Kirchhausen T, Chen J, Ploegh HL. T-cell engagement of dendritic cells rapidly rearranges MHC class II transport. *Nature* 2002;418:983–988.
37. Raposo G, Nijman HW, Stoorvogel W, Liejendekker R, Harding CV, Melief CJ, Geuze HJ. B lymphocytes secrete antigen-presenting vesicles. *J Exp Med* 1996;183:1161–1172.
38. Wubbolts R, Fernandez-Borja M, Oomen L, Verwoerd D, Janssen H, Calafat J, Tulp A, Dusseljee S, Neefjes J. Direct vesicular transport of MHC class II molecules from lysosomal structures to the cell surface. *J Cell Biol* 1996;135:611–622.
39. Gluschankof P, Suzan M. HIV-1 Gag polyprotein rescues HLA-DR intracellular transport in a human CD4 (+) cell line. *Virology* 2002;300:160–169.
40. Stoorvogel W, Kleijmeer MJ, Geuze HJ, Raposo G. The biogenesis and functions of exosomes. *Traffic* 2002;3:321–330.
41. Littman DR. Chemokine receptors: keys to AIDS pathogenesis? *Cell* 1998;93:677–680.
42. Finke D, Acha-Orbea H. Immune response to murine and feline retroviruses. In: Pantaleo G, Walker BD, eds. *Retroviral Immunology*. Totowa, N.J. Humana Press; 2001. pp 125–157.
43. Meltzer MS, Skillman DR, Gomas PJ, Kalter DC, Gendelman HE. Role of mononuclear phagocytes in the pathogenesis of human immunodeficiency virus infection. *Annu Rev Immunol* 1990;8:169–194.
44. Geijtenbeek TB, Kwon DS, Torensma R, van Vliet SJ, van Duijnhoven GC, Middel J, Cornelissen IL, Nottet HS, Kew I, Ramani VN, Littman DR, Figdor CG, van Kooyk Y. DC-SIGN, a dendritic cell-specific HIV-1-binding protein that enhances trans-infection of T cells. *Cell* 2000;100:587–597.
45. Kwon DS, Gregorio G, Bitton N, Hendrickson WA, Littman DR. DC-SIGN-mediated internalization of HIV is required for trans-enhancement of T cell infection. *Immunity* 2002;16:135–144.
46. McDonald D, Wu L, Bohks SM, KewalRamani VN, Unutmaz D, Hope TJ. Recruitment of HIV and its receptors to dendritic cell–T cell junctions. *Science* 2003;300:1295–1297.
47. Pelchen-Matthews A, Kramer B, Marsh M. Infectious HIV-1 assembles in late endosomes in primary macrophages. *J Cell Biol* 2003;162:443–455.
48. Campbell RE, Tour O, Palmer AE, Steinbach PA, Baird GS, Zacharias DA, Tsien RY. A monomeric red fluorescent protein. *Proc Natl Acad Sci USA* 2002;99:7877–7882.
49. Kayman SC, Park H, Saxon M, Pinter A. The hypervariable domain of the murine leukemia virus surface protein tolerates large insertions and deletions, enabling development of a retroviral particle display system. *J Virol* 1999;73:1802–1808.
50. Masuda M, Kakushima N, Wilt SG, Ruscetti SK, Hoffman PM, Iwamoto A. Analysis of receptor usage by ecotropic murine retroviruses, using green fluorescent protein-tagged cationic amino acid transporters. *J Virol* 1999;73:8623–8629.
51. Martinez I, Chakrabarti S, Hellevik T, Morehead J, Fowler K, Andrews NW. Synaptotagmin VII regulates Ca²⁺-dependent exocytosis of lysosomes in fibroblasts. *J Cell Biol* 2000;148:1141–1149.
52. Barbero P, Bittova L, Pfeffer SR. Visualization of Rab9-mediated vesicle transport from endosomes to the trans-Golgi in living cells. *J Cell Biol* 2002;156:511–518.
53. Blott EJ, Bossi G, Clark R, Zvelebil M, Griffiths GM. Fas ligand is targeted to secretory lysosomes via a proline-rich domain in its cytoplasmic tail. *J Cell Sci* 2001;114:2405–2416.
54. Kanai F, Liu H, Field SJ, Akbary H, Matsuo T, Brown GE, Cantley LC, Yaffe MB. The PX domains of p47phox and p40phox bind to lipid products of PI(3)K. *Nat Cell Biol* 2001;3:675–678.
55. Sonnichsen B, De Renzis S, Nielsen E, Rietdorf J, Zerial M. Distinct membrane domains on endosomes in the recycling pathway visualized by multicolor imaging of Rab4, Rab5, and Rab11. *J Cell Biol* 2000;149:901–914.
56. Girotti M, Banting G. TGN38-green fluorescent protein hybrid proteins expressed in stably transfected eukaryotic cells provide a tool for the real-time, *in vivo* study of membrane traffic pathways and suggest a possible role for ratTGN38. *J Cell Sci* 1996;109:2915–2926.
57. Barsov EV, Payne WS, Hughes SH. Adaptation of chimeric retroviruses *in vitro* and *in vivo*: isolation of avian retroviral vectors with extended host range. *J Virol* 2001;75:4973–4983.

58. Yueh A, Goff SP. Phosphorylated serine residues and an arginine-rich domain of the Moloney murine leukemia virus p12 protein are required for early events of viral infection. *J Virol* 2003;77:1820–1829.
59. Folsch H, Pypaert M, Schu P, Mellman I. Distribution and function of AP-1 clathrin adaptor complexes in polarized epithelial cells. *J Cell Biol* 2001;152:595–606.
60. Taguchi T, Pypaert M, Warren G. Biochemical sub-fractionation of the mammalian Golgi apparatus. *Traffic* 2003;4:344–352.
61. Erlwein O, Buchholz CJ, Schnierle BS. The proline-rich region of the ecotropic Moloney murine leukaemia virus envelope protein tolerates the insertion of the green fluorescent protein and allows the generation of replication-competent virus. *J Gen Virol* 2003;84:369–373.